Asymmetric sulfoxidation of thioether catalyzed by soybean pod peroxidase：kinetic model

Yuanyuan Zhang[1,2*], Huiling Li[1], Zhiyong Wang[3], Depeng Li[3], Xin Gao[3,4*]

1 State Key Laboratory Base for Eco-Chemical Engineering in College of Chemical Engineering, Qingdao University of Science and Technology, Mailbox 70, 53 Zhengzhou Road, Qingdao 266042, China

2 William G. Lowrie Department of Chemical and Biomolecular Engineering, Ohio State University, 151 West Woodruff Avenue, Columbus, Ohio 43210, USA

3 Department of Pharmaceutical Engineering, College of Chemical Engineering, Qingdao University of Science and Technology, Mailbox 70, 53 Zhengzhou Road, Qingdao 266042, China

4 Kekulé-Institut für Organische Chemie und Biochemieder Rheinischen Friedrich-Wilhelms-Universität Bonn Gerhard-Domagk-Str. 153121 Bonn Germany

A B S T R A C T

The asymmetric sulfoxidation catalyzed by soybean pod peroxidase (SPP) in water-in-oil microemulsions were carried out with the yield of 91.56% and e.e of 96.08% at the activity of SPP of 3200 U ml^{-1} and 50°C for 5 h. The mechanism with a two-electron reduction of SPP-I is accompanied with a single-electron transfer to SPP-I and nonenzymatic reactions, indicating that three concomitant sub-mechanisms contribute to the asymmetric oxidation involving five enzymatic and two nonenzymatic reactions, which can represent the asymmetric sulfoxidation of organic sulfides to form enantiopure sulfoxides. With 5.44% of the average relative deviation, a kinetic model fitting experimental data very well was developed. The enzymatic reactions may follow ping-pong mechanism with substrate inhibition of H_2O_2 and product inhibition of esomeprazole, while nonenzymatic reactions, a power law. Those results indicate that SPP with a lower cost and higher thermal stability may be

*Corresponding author at: Department of Pharmaceutics, Qingdao University of Science and Technology, 53 Zhengzhou Road, 266042 Qingdao, China.
*E-mail: yangfengk@163.com (F.Yang); 523985377@qq.com (X.Gao)

used as an effective substitute for Horseradish Peroxidase.

Keywords: Kinetic model, soybean pod peroxidase, asymmetric sulfoxidation, chiral sulfoxides, substrate inhibition

1.Introduction

Peroxidases are oxidoreductases containing heme which can catalyze the oxidizing various organic compounds including thioamidines, thioanisoles, and phenols in the presence of hydrogen peroxide[1–7]. Soybean pod peroxidase (SPP) is a peroxidase extracted from soybean pods which are one of the most abundant natural resources in the world with higher production than soybean shells from which the soybean hull peroxidase (SHP) can be extracted. Over the years, there have been many reports on the mechanism of oxidation catalyzed by peroxidase. There are two main modes of oxygen transfer from the intermediary complex, which is yielded by the heterolytic cleavage of the hydroperoxide bond to the sulfide[8–10], as follows: (1) a one-step oxygen transfer mechanism involving a two-electron reaction and (2) a two-step oxygen transfer mechanism including a radical cation intermediate[11–13]. However, it is important for further insight into the mechanism of oxidation catalyzed by peroxidase for the process development. Chiral sulfoxides have been widely used as chiral intermediates, ligands, and pharmaceuticals such as proton pump inhibitors (PPI)[14,15]. Esomeprazole with chiral sulfoxides structure, S-enantiomer of omeprazole, is an important member of the PPI family which is used to treat gastric ulcer disease. It has been reported that the active S-enantiomer has obvious therapeutic advantages over the racemate because of its stereoselective pharmacokinetics[14,15]. So far, chiral sulfoxides are mainly produced using chemical asymmetric oxidizing of sulfides with many drawbacks, especially environmental damage[16,17]. Monooxygenase has been used for asymmetric sulfoxidation[18,19], however, it has a disadvantage of requiring a cofactor cycling system. On the contrary, peroxidase can catalyze oxidation without using cofactor. Xu et.al. has carried out extensive and in-depth research for bio asymmetric sulfoxidation using cell[20] and enzyme[21,22]. Enantioselective oxidation of

sulfides catalyzed by engineering Acinetobacter calcoaceticus cyclohexanone monooxygenases was successfully conducted with a glucose dehydrogenase for recycling cofactor NADPH[22]. Asymmetric sulfoxidation catalyzed by peroxidases is thus very important biotransformation to produce chiral sulfoxides etc[23–26]. Up to now, according to our best knowledge, it has not been reported that chiral sulfoxide esomeprazole is produced using asymmetric sulfoxidation catalyzed by peroxidases including SPP.

Microemulsions are thermodynamically stable, isotropic, and transparent dispersions of oil and water with a droplet size of 10-100 nm, which were formed by interfacial films of surfactant and cosurfactant[27,28]. Microemulsion is an excellent reaction medium for enzyme catalysis in which enzymes exist in the water phase while hydrophobic substrates and products in the oil phase[29]. Remarkable effects of the interfacial film on the enzymatic activity were observed in microemulsions[30,31]. In the present work, water-in-oil microemulsions were thus employed as reaction mediums because of hydrophobic substrates and products.

Kinetic modeling provides insight into the mechanism for the oxidation of sulfides catalyzed by peroxidase to enantiopure sulfoxides, which can be applied to the analysis of the reaction process and the mathematical model scale-up of reactors producing enantiopure sulfoxides. A few works of establishing the kinetic model for the oxidation of thioether catalyzed by peroxidases have been reported. Based on one-step and two-step oxygen-transfer reaction mechanisms, two initial velocity equations were established[13], however, the ability of the initial velocity equation to represent the kinetic behavior is significantly weak. In the early years, the initial velocity equation was often used, because it required very simple data processing, whereas the differential kinetics experiment with great difficulty and poor experimental accuracy must be conducted to obtain initial velocity data. A simple kinetic equation based on pseudo-first-order was developed using transient-state kinetic data[32]. The oxidation of guaiacol catalyzed by HRP was carried out in a water-miscible ionic liquid, and a Michaelis–Menten equation of single substrate with non-competitive inhibition was

adopted, in which the ionic liquid was a weak inhibitor[33,34]. However, hydrogen peroxide was not considered as a substrate in the kinetic equation. A comprehensive study for rice peroxidase (RP) was performed in order to confirm the feasibility of RP as a substitute for HRP, and their kinetic studies based on the oxidation of both guaiacol and dopamine with H_2O_2 catalyzed by RP in organic solvents indicate that RP obeyed Michaelis–Menten kinetics[10].

Obviously, the research in kinetic modeling for the oxidation of sulfides catalyzed by peroxidase to enantiopure sulfoxides is insufficient in extent and intensity, and more research should be carried out. To develop the enzymatic process and deeper insight into the mechanism for the oxidation of sulfides catalyzed by peroxidase, it is necessary to establish a kinetic model under this complex reaction system with multiple reactions where the product of one reaction may be the substrate of another one[35]. King-Altman method must be employed to establish the kinetic model.

In the present work, SPP-catalyzed asymmetric sulfoxidation of omeprazole thioether in water-in-oil microemulsions was carried out for the synthesis of enantiopure sulfoxide esomeprazole This may be a potential green technology considering no cofactor needed and commercially availability of SPP at low cost. Herein, a reaction mechanism was explored and a kinetic model of the asymmetric sulfoxidation involving seven reactions was developed, in which the numerical solution of ordinary differential equations is coupled with an optimization algorithm to identify the model parameters.

2.Materials and Methods

2.1Materials

PEG4000, anhydrous ethanol, Cetyltrimethylammonium bromide (CTAB), hydrogen peroxide (30%) (A), n-butanol, isooctane, and methanol were purchased from Sinopharm Group Chemical Reagent Co., Ltd., China, respectively. All the above reagents were of analytical purity and were used directly without further purification. 5-methoxy-2-(((4-methoxy-3,5-dimethylpyridin-2-yl)methyl)thio)-1H-

benzoimidazole (Omeprazole thioether, B) was purchased from Jinan Ward Chemical Co., Ltd., China, (S)- 5-Methoxy-2-[(4-methoxy-3,5-dimethylpyridin-2-yl)methylsulfinyl]-3H-benzoimidazole ((S)-omeprazole, PS) from Suzhou Vita Chemical Co., Ltd., China, 5-Methoxy-2-[(4-methoxy-3,5-dimethylpyridin-2-yl)methylsulfinyl]-1H-benzoimidazole (omeprazole) from Shandong Shouguang Fukang Pharmaceutical Co., Ltd and fresh soybean pods were purchased from an urban supermarket.

2.2 Separation and purification of soybean pod peroxidase

Fresh soybean pods were soaked by 1.3-fold volume phosphate buffer (pH6.8) at 4℃ and then smashed using a high-speed food mixer at 15000 rpm. The obtained soybean pods smashed were extracted 2 h in phosphate buffer (pH6.8), and filtered with a 500-mesh filter cloth. The filtrate was then separated and purified as follows: impurities removal by zinc ion, extraction with an aqueous two-phase system (PEG 4000, 12%, w/w /K2HPO4, 13%, w/w), ultrafiltration, gel filtration chromatography with Sephadex G-75 and DEAE ion-exchange chromatography, respectively. Finally, the resulted concentrated extract was lyophilized and the soybean pod peroxidase powder was obtained with 160 U mg^{-1}. The purified SPP powder was used for catalysis of the sulfoxidation for the first time.

2.3 Peroxidase -catalyzed sulfoxidation of omeprazole sulfide in reverse micelles to prepare chiral sulfoxide

A peroxidase-catalyzed sulfoxidation of omeprazole sulfide in water-in-oil microemulsions was carried out in a volumetric flask of 20 ml. A typical CTAB/isooctane/n-butanol/water microemulsion with WO of 16 was prepared by weighing and adding the amounts of CTAB (1.265g), isooctane (7.8ml), n-butanol (1.2ml), totaling 1ml of phosphate buffer solution (pH 6.0) and a certain amount of SPP powder to yield a final concentration of peroxidase from 240 to 3200Uml^{-1} and omeprazole sulfide, 20 mM, respectively. The sulfoxidation was initiated by adding

hydrogen peroxide to the water-in-oil microemulsion which was incubated at 50°C in a water bath shaker with 150 rpm for 5 h. The reaction was stopped by adding 3-fold distilled water into the reaction solution, and then the mixture was separated by centrifugation to organic phase and aqueous phase. The latter was extracted with ethyl acetate and the combined organic phase was taken for HPLC analysis of the e.e and conversion, while the former was used to assay the SPP activity.

2.4 Assay of SPP activity

Assay of SPP activity was conducted based on a colouring reaction of 4-aminoantipyrine and phenol with H_2O_2 in phosphate buffer (pH 7.0), monitored by a spectrophotometer at 510nm[1]. One unit of SPP activity (U) represents the change of absorbance value for 5 min at 510 nm and 25 ℃ in a quartz cuvette (1cm), in which the increase in absorbance was collected with a UV-2550 spectrophotometer (Shimadzu, Japan).

2.5 HPLC analysis

For HPLC analysis of e.e and conversion, samples were taken from the reaction solution at specific time intervals and phase separation was performed by adding three-fold distilled water into the sample. The resulted organic phase was used for HPLC analysis and the aqueous phase was used to determine the residual activity of SPP. For HPLC analysis of hydrogen peroxide, samples were taken from the reaction solution and directly used for HPLC analysis. The conversion of omeprazole thioether, enantiomeric excess (e.e), the yields of (S)-omeprazole and (R)-omeprazole were analyzed by a chiral HPLC system with Agilent 1200 LC (Agilent Technologies, Inc., and Santa Clara USA) with a diode array detector. The column equipped with a chiral column Amylose-SA (250× 4.6mm, 5um, YMC, Japan) was maintained at 30 °C and the detection wavelength was 302 nm. The sample volume was 20 μL and the mobile phase was a 15:85 (v/v) acetonitrile: phosphate buffer (pH6.0) mixture at a flow rate of 0.6 $mLmin^{-1}$. The retention times for (S)-omeprazole and (R)-omeprazole were 5.8 and 6.9 min, respectively. Hydrogen peroxide was determined by HPLC with

an Inertsil ODS-SP column (150×4.6mm, 5μm). The mobile phase for hydrogen peroxide analysis was a mixture of methanol and water with a ratio of 2:8 and the detection wavelength was 220 nm at a flow rate of 0.5 ml min^{-1}, and other conditions were the same as described above. The retention time for hydrogen peroxide was 3.7 min.

3.Model development

3.1 Peroxidase- catalyzed reaction mechanism and modeling

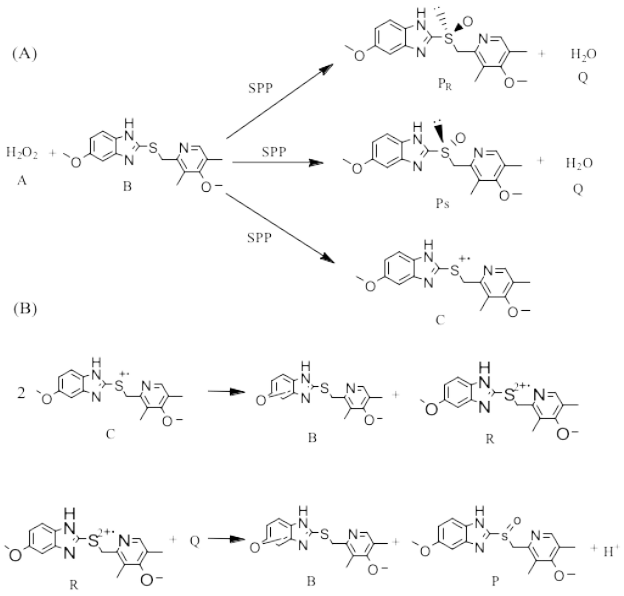

Scheme 1. Asymmetric sulfoxidations of omeprazole thioether catalyzed by soybean pod peroxidase for the production of enantiopure esomeprazole P_S. (A) Enzymatic reactions; (B) Chemical reactions.

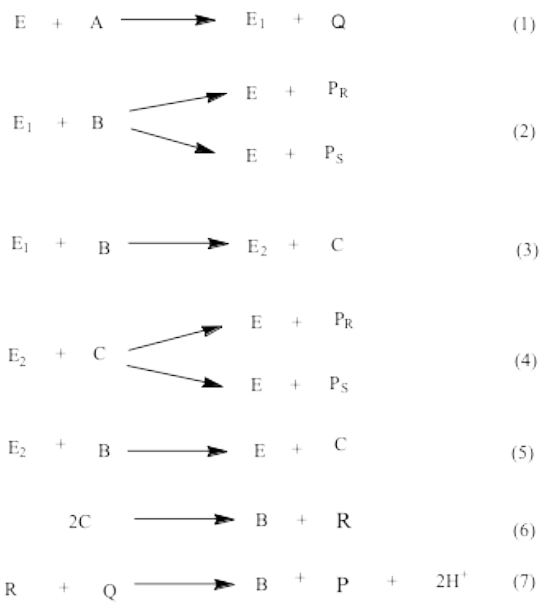

Scheme 2. The proposed sequence of reactions for the peroxidase-catalyzed asymmetric sulfoxidation of thioether to form chiral sulfoxide.

Scheme 1 shows the proposed reaction pathway for asymmetric oxidation of the thioamidine (omeprazole thioether) catalyzed by soybean pod peroxidase for the production of the chiral sulfoxide (enantiopure esomeprazole), and there are five enzymatic reactions and two nonenzymatic reactions included in the chemoenzymatic reaction system. Furthermore, the reaction mechanism proposed of peroxidase-catalyzed asymmetric oxidation of thioether is shown in Scheme 2. Reactions 1 and 2 form a reaction group 1 in which the thioamidine is asymmetric oxidized to the chiral sulfoxide catalyzed by SPP (E), while reactions 1, 3 and 4 form a reaction group 2 in which SPP is converted to SPP-I(E_1), then SPP-II (E_2), the thioamidine is converted to thioamidine cation radicals which are converted to the enantiopure sulfoxide by SPP-II. The reaction group 3 is composed of reactions 1, 3 and 5, in which the thioamidine cation radical is generated in the peroxidase-catalyzed reaction. In reactions 6 and 7, two thioamidine cation radicals react to yield thioamidine dication radicals which react with water to generate racemic sulfoxides in a nonenzymatic fashion.

In reaction 1 H_2O_2 binds to E, resulting in quickly generating water and converting E into E_1. Therefore, it is reasonable to consider this reaction is irreversible. Reactions 2 and 4 are oxidation reactions which generally speaking are

irreversible. In reactions 3 and 5, cation radicals are generated and the reactions should be irreversible. In reaction 6, two thioamidine cation radicals react to form thioamidine dication radicals which react to form sulfoxides in reaction 7, and reactions 6 and 7 are also considered as irreversible.

In the chemoenzymatic system, there are four substrates (A, B, C, and Q) and five products (B, C, H^+, Q, P_R, and P_S), and among them, B, C, and Q are not only substrates of reactions 2-6 but also products of reactions 1, 3, 5 and 6, respectively.

Loss of the SPP activity can't be neglected in the oxidation because there was a large loss of the activity after one run in our preliminary experiments. In the present study, the residual activity was correlated with time as follows: $E= E_0 \exp(-0.127t)$. Details for the correlation can be found in the section of results and discussion.

There are many studies on the mechanism of the lipase-catalyzed reaction, but a few on peroxidase. It is generally believed that many reactions catalyzed by enzymes obey one of the following two mechanisms: (1) Ping-pong mechanism[36–38] and (2) Sequential mechanism[39–42]. The oxidation of sulfides catalyzed by peroxidase to enantiopure sulfoxides involves two intermediate forms of peroxidase: compounds I and II, which can actually be thought of as changing patterns of the peroxidase. We may thus presume that the reaction may be subject to the ping-pong mechanism. The mechanism of the peroxidase-catalyzed asymmetric sulfoxidation is discussed as follows.

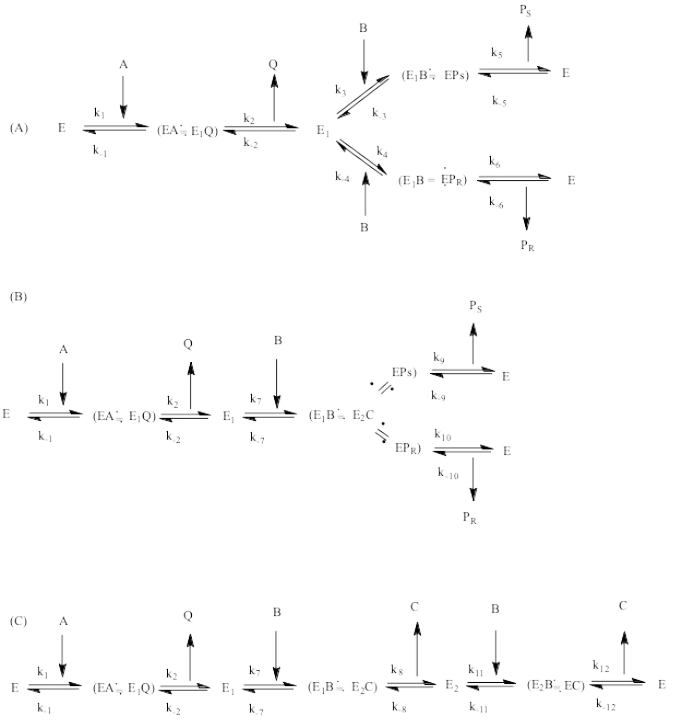

Scheme 3. The schemata of the ping-pong bi-bi mechanism proposed for the peroxidase-catalyzed asymmetric sulfoxidation of thioether to form chiral sulfoxide.

As shown in scheme 3 (A), for reactions 1 and 2 a ping-pong mechanism of the peroxidase-catalyzed oxidation of the thioether to the chiral sulfoxide is discussed as follows. For reaction 1, first, substrate A catches with peroxidase E to form EA, EA then transforms to E_1Q in which Q is a leaving group. The leaving group Q is released from E_1Q and E_1 then catches with B to yield peroxidase complex E_1B, indicating one of the characteristics of ping-pong mechanism. For reaction 2 the asymmetric sulfoxidation occurs: E_1 binds to substrate B to yield peroxidase complex E_1B, and most of the products are EP_S, and a small amount is EP_R because the enantioselectivity of SPP prefers S configuration in water. Finally, the products P_R and P_S are released from the peroxidase complexes and E_1 regenerates into its original form E.

For reactions 1, 3 and 4 as shown in scheme 3 (B), then, the reactions may obey the ping–pong mechanism because there is a leaving group Q in reaction 1. The asymmetric oxidation takes place, E_1 binds B to yield the peroxidase complex E_1B in which E_1 changes to E_2. The prochiral molecule B is converted to C, omeprazole

sulfide cation, which is then oxidized to a large amount of P_S and a small amount of P_R, respectively, and E_2 restores to E when both P_S and P_R are released from the enzyme complex E_2P_S or E_2P_R.

Finally, for reactions 1, 3 and 5 C is formed in both reactions 3 and 5. For reaction 3 the interaction of peroxidase with B makes E_1B become E_2C, then C leaves from E_2C, and E_2 is released and binds to B to yield peroxidase complex E_2B, E_2 interacting with B makes E_2B become EC in reaction 5, C is released from EC and E_2 restores to original E as shown scheme 3(C). Omeprazole sulfide cation C formed here will participate in the following reactions 6 and 7.

E, E_1, and E_2 are referred to as protoenzyme, compound I and compound II, and the last two are changed patterns of the protoenzyme[9,43–45] or R-PorFe^{II}, R-$^{+\cdot}$PorFe^{IV}=O, and R-PorFe^{IV} = O[46] and SPP, SPP-I and SPP-II, similar to HRP, HRP-I, and HRP-II[9] , respectively. A variety of spectroscopic methods have been employed to characterize both HRP-I and II[47–50]. Compound I and II have also been confirmed by the experimental results of transient-state kinetics[32] .

Reaction 6 and 7 are nonenzymatic reactions and a power law was adopted as their kinetic equations in which products are racemic, i.e. P_S is equal to P_R.

Moreover, substrate and product inhibition on enzyme often occur in enzymatic catalyzed reactions, which may significantly influence the kinetic behavior of the reactions, resulting in that the kinetic model of the reactions will change accordingly[51,52]. Therefore, substrate and product inhibition will be considered in the establishment of the peroxidase-catalyzed reaction kinetic model. In the chemoenzymatic reaction system, peracetic acid, hydrogen peroxide, and omeprazole thioether might have substrate inhibition on peroxidase, while (S)-omeprazole may have product inhibition on peroxidase, but the inhibition of (R)-enantiomer is ignored because its concentration is much lower than (S)-enantiomer. Thus hydrogen peroxide and omeprazole thioether were considered as substrate inhibitors and (S)-omeprazole as a product inhibitor in the kinetic model development. For the kinetic equations,

substrate inhibition is indicated as $K_i*S_i*S_i$ and product inhibition is expressed as K_i*P_i.

Furthermore, both substrate inhibition and product inhibition are elaborated. With substrate A as an example, the mechanism of substrate inhibition is discussed as follows. The binding of substrate inhibitor A to peroxidase complexes, such as EA, E_1B, E_2C, results in the formation of inactive dead-end complexes, such as AEA, AE_1B, and AE_2C. The inhibitor binds to the unbound enzyme as well as the enzyme-substrate complex, resulting in the substrate inhibition. Consequently, the resulting dead-end complex cannot further react to produce the desired target product although the substrate can still bind to the enzyme or enzyme complex[53]. Similar to substrate inhibition, product inhibitor P_S catches with EB, EP_S, and EQ to form inactive dead-end enzyme complexes P_SEB, P_SEP_S and P_SEQ, respectively, which hinder product forming and substrate converting.

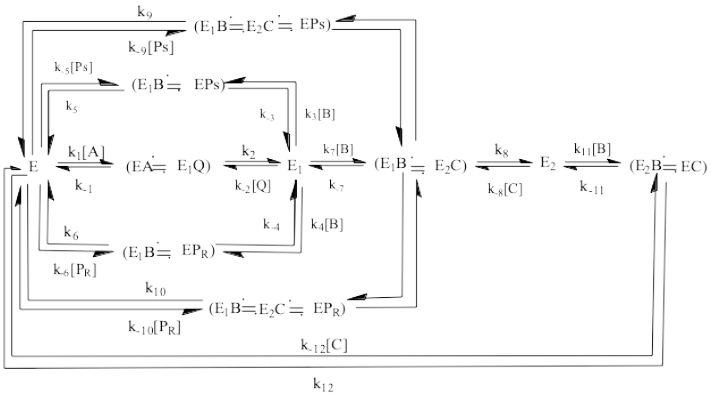

Scheme 4. The King-Altman schemata of the ping-pong Bi-Bi mechanism proposed for the peroxidase-catalyzed sulfoxidation of thioether to form chiral sulfoxide. For simplicity, schemes of substrate and product inhibition are not given.

Based on the above basic discusses of the reaction mechanism of the asymmetric oxidation of the thioether catalyzed by SPP for the production of enantiopure sulfoxide and the model of the asymmetric oxidation was developed. In this work, the kinetic model was established using the King-Altman approach. Scheme 4 shows the King-Altman schemata of the kinetic mechanism of the asymmetric oxidation. As mentioned earlier, the last step of several reactions is irreversible. However, the King-

Altman schemata are still drawn according to the reversible reaction. The reversible terms are removed from the kinetic rate equations when the equations are derived, thus, only the terms of forwarding steps still remain in the rate equations established. The details of both substrate and product inhibition were not given in the scheme for simplicity, and after a lot of deduction, merging and simplification, the kinetic rate equations (8-23) for substrates and products in reactions 1-7 were derived, which are the differential equations expressed as follows:

$$KK1=K_1+K_2\times Y(1)\times A_0+K_3\times Y(2)\times B_0+K_4\times Y(1)\times A0\times Y(2)\times B_0+K_5\times Y(1)\times A_0\times Y(1)\times A_0+K_6\times Y(3)\times B_0+K_7\times Y(2)\times B_0\times Y(2)\times B_0 \quad (8)$$

$$KK2=KK1+ K_8\times Y(1)\times A_0\times Y(2)\times B_0\times Y(2)\times B_0 \quad (9)$$

$$E=E_0\times\exp(-0.127\times t) \quad (10)$$

$$EK1=E/KK1 \quad (11)$$

$$EK2=E/KK2 \quad (12)$$

$$dY(1)/dt= -K_{11}\times Y(1)\times Y(2)\times B0\times Y(2)\times B_0\times EK1 \quad (13)$$

$$dY(2)/dt=-K_{12}\times Y(1)\times A_0\times Y(2)\times EK1-K_{13}\times Y(1)\times A0\times Y(2)\times B_0\times Y(2)\times EK2-K_{14}\times Y(1)\times A_0\times Y(2)\times EK1+ K_{18}\times(Y(6) \times B_0)\text{^}K_{19}/B_0 \quad (14)$$

$$dY(3)/dt=K_{14}\times Y(1)\times A_0\times Y(2)\times EK1+K_{15}\times Y(1)\times A_0\times Y(2)\times B_0\times Y(5)\times EK2+K_{18}\times(Y(6)\times B_0)\text{^}K_{19}/B_0 \quad (15)$$

$$dY(4)/dt=K_{16}\times Y(1)\times A_0\times Y(2)\times EK1+K_{17}\times Y(1)\times A_0\times Y(2)\times B_0\times Y(5)\times EK2+K_{18}\times(Y(6)\times B_0)\text{^}K_{19}/B_0 \quad (16)$$

$$dY(5)/dt=K_{12}\times Y(1)\times A_0\times Y(2)\times EK1+K_{13}\times Y(1)\times A_0\times Y(2)\times B_0\times Y(2)\times EK2-K_{15}\times Y(1)\times A_0\times Y(2)\times B_0\times Y(5)\times EK2-2\times K_9\times(Y(5)\times B_0)\text{^}(2\times K_{10})/B_0 \quad (17)$$

$$dY(6)/ dt= -K_{18}\times(Y(6) \times B_0)\text{^}K_{19}/B_0+ K_9\times(Y(5)\times B_0)\text{^}(2\times K_{10})/B_0 \quad (18)$$

$$dY(7)/ dt= K_{14}\times Y(1)\times A_0\times Y(2)\times EK1 \quad (19)$$

$$dY(8)/dt= K_{15}\times Y(1)\times A_0\times Y(2)\times B_0\times Y(5)\times EK2 \quad (20)$$

$$dY(9)/dt= K_9\times(Y(5)\times B_0)\text{^}(2\times K_{10})/B_0 \quad (21)$$

$$dY(10)/dt= K_{16}\times Y(1)\times A_0\times Y(2)\times EK1 \quad (22)$$

$$dY(11)/dt= K_{17}\times Y(1)\times A_0\times Y(2)\times B_0\times Y(5)\times EK2 \quad (23)$$

where A_0, B_0, and E_0 were initial concentrations of hydrogen peroxide, (S)-omeprazole and peroxidase, respectively; Y(1)-Y(6) are relative residual or yield of A, B, C, P_S, P_R, and R, respectively. Eqs 19-23 are for the convenience and intuitive

analysis of the simulation results of the reaction kinetics model which are not necessary for solving the reaction kinetics model. Eqs 19, 20 and 21 show the rate at which P_S is generated by reactions 1, 3 and 4, respectively and eqs 22 and 23 show P_R, by reactions 1 and 3, respectively. $K_5\times Y(1)\times A_0\times Y(1)\times A_0$ and $K_7\times Y(2)\times B_0\times Y(2)\times B_0$ represent the substrate inhibition terms of A and B, respectively, while $K_6\times Y(3)\times B_0$, the product inhibition term of P_S.

In addition to the above basic considerations regarding the reaction mechanisms for the chemoenzymatic dynamic covalent kinetic resolution, there are other factors including substrate inhibition, competitive inhibition and non-competitive inhibition, which may significantly influence the kinetic behavior of reactions, resulting in that the kinetic model of reactions will change accordingly. Thus, these factors will be taken into account in subsequently establishing and identifying the kinetic model.

3.2 Estimation of kinetic Model Parameters

With the experimental data of asymmetric sulfoxidation of the thioether to form the enantiopure sulfoxide, in order to identify the kinetic model, the kinetic model parameters of equations (8)-(23) were estimated using coupling ordinary differential equations solver with an optimization method, and the kinetic model was used to fit the kinetic experimental data by the minimum of the equation 24[38]:

$$F=\sum\sum abs((Y^{simul.}_{ij}-Y^{exp}_{ij})/Y^{simul.}_{ij}) \qquad (24)$$

As shown in equation (24), the absolute deviation between the model simulated data and the experimental data were used although the square of deviation is often used to calculate the deviation between two values, resulting in avoiding the increase of nonlinearity caused by the sum of squares of deviations. Using the software Matlab 2019b, the model parameters were estimated in which the kinetic rate equations (8)-(23) were solved using function ode45, while function fmincon was used to solve equation (24).

4.Results and discussion

4.1 Residual activity of soybean pod peroxidase after one run

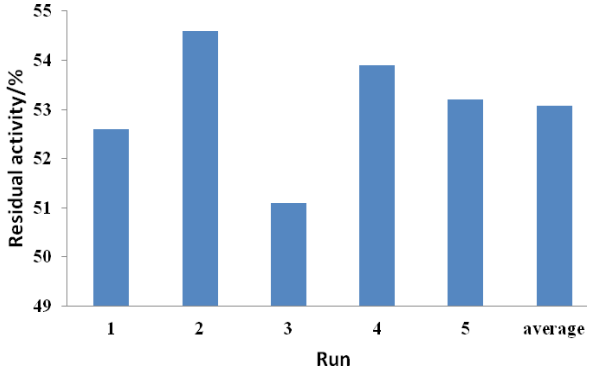

Fig. 1 Residual activity of soybean pod peroxidase vs. run

Temperature, 48°C, stirring speed,150 rpm, E_0=480 U ml^{-1}.

Figure 1 gives the residual activity of soybean pod peroxidase after one run and the average was about 53%. Thus, loss of activity of soybean pod peroxidase must be taken into account in developing the kinetic model. Hydrogen peroxide in the chemoenzymatic asymmetric oxidation system may deactivate soybean pod peroxidase to some extent.

Hydrogen peroxide has a disadvantageous effect on enzyme stability which can inactivate the peroxidase[54]. The deactivation process of peroxidase in the enzyme-catalyzed oxidation consists of two stages: the formation of compound III which is followed by the accumulation of irreversibly deactivated peroxidase[55]. Slow enzyme inactivation would occur if the enzyme is exposed to a high concentration of hydrogen peroxide[56]. Enzyme inactivation is a gradual process with time, and eventually, the oxidation process leads to disruption of the enzyme disulfide bond and loss of protein primary structure[57–59].

The exponential correlation between the soybean pod peroxidase activity and time was adopted as follows:

$$E=E_0*\exp(-0.127t) \qquad (25)$$

where 0.127 is the rate constant of the soybean pod peroxidase inactivation, i.e. the slope of the enzyme inactivation curve vs. time. Eq. (25) was applied to the kinetic model for the enzyme activity, which fitted the experimental data very well, demonstrating that the simple exponential connection is reasonable. In this study, the

reaction temperature of SPP was 50 ℃, while the usual temperature range of HRP is 20-30 ℃, so the thermal stability of SPP is much higher than HRP.

4.2 Asymmetric sulfoxidation and reaction mechanism

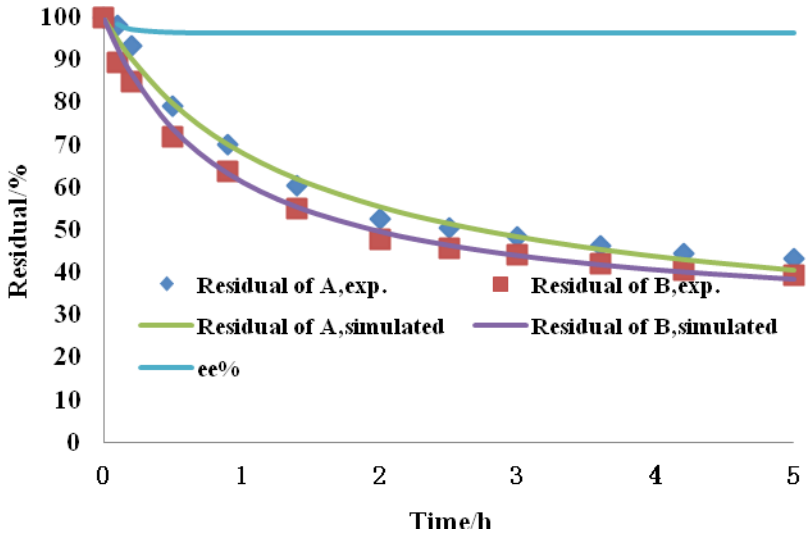

Fig. 2 Residual of A and B in simulated and experimental data vs. time Temperature, 50°C, stirring speed,150 rpm, E_0=480 U ml^{-1}.

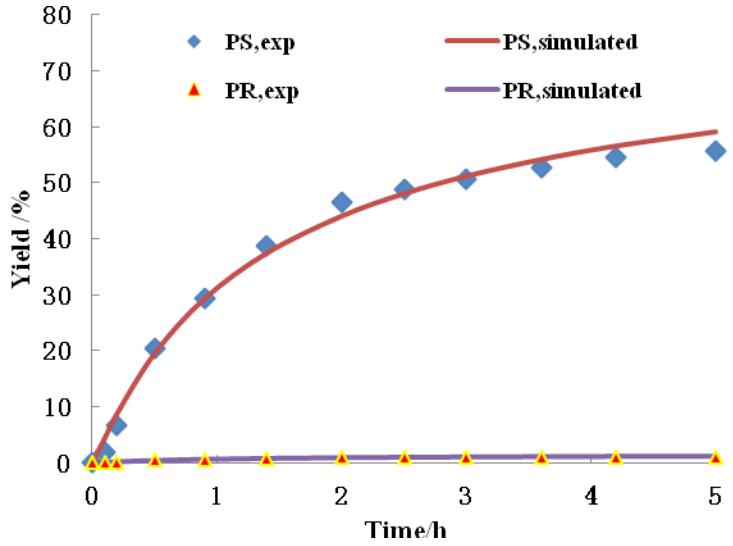

Fig. 3 Comparison of the simulated and experimental yield of P_S and P_R

Temperature, 50°C, stirring speed,150 rpm, E_0=480 U ml^{-1} ，the corresponding concentration of peroxidase, 20 mg U ml^{-1}.

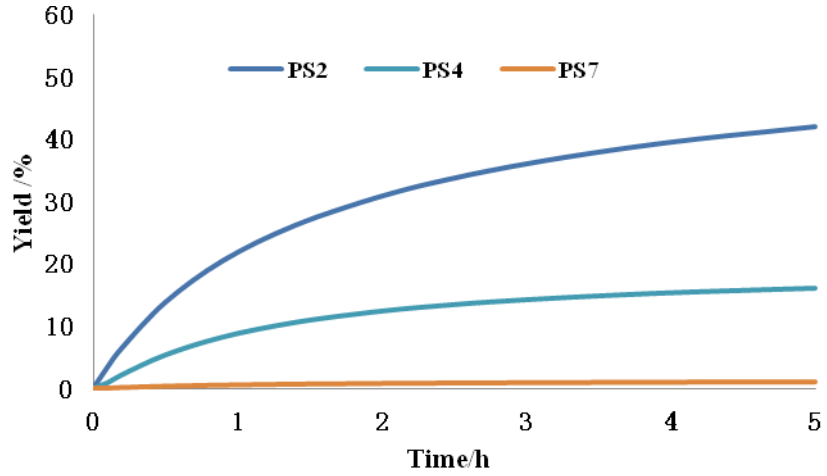

Fig. 4 The contribution of reactions 2, 4 and 7 to P_S, Ps= P_{S2} +P_{S4} +P_{S7}

Temperature, 50°C, stirring speed,150 rpm, E_0=480 U ml^{-1}.

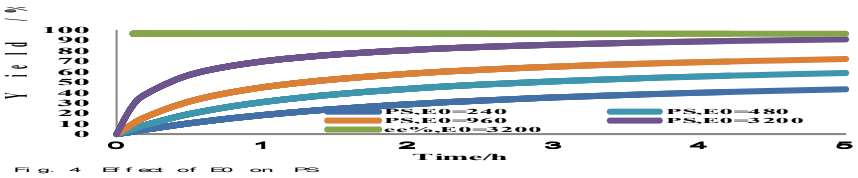

Fig. 5 Effect of initial activity of peroxidase E_0 on the yield of P_S

Temperature, 50°C, stirring speed,150 rpm ，ee (5 h), 96.08%, P_S(5 h), 91.56%. For E_0=3200 U ml^{-1}, the corresponding concentration of peroxidase was 20 mg U ml^{-1}.

The experiment of asymmetric sulfoxidation of thioether catalyzed by SPP for the production of the enantiopure sulfoxide in the water-in-oil microemulsion was carried out successfully. Fig. 2 shows the comparisons of simulated results and experimental data for substrates A and B, while Fig. 3, for products P_S and P_R with the initial concentration of peroxidase E_0 of 480 U ml^{-1}.

P_S is the result of three concomitant reactions, and computer simulations based on the model established which enables us to distinguish the contribution of reactions 2, 4 and 7 to the yield. As shown in Fig. 4, reaction 2 contributes the most, reaction 4 the second, and reaction 7 the least which is very small in fact. Considering that both reactions 2 and 4 are enzymatic reactions, we speculated that the yield may be further improved if the initial concentration of peroxidase is increased. As expected, the yield P_S increased from 59.1% to 91.56% and e.e decreased slightly from 96.23% to 96.08%, respectively, with the increase of the initial concentration of peroxidase from 480 U ml^{-1} to 3200 U ml^{-1} (the corresponding concentration of peroxidase was 20 mg U ml^{-1}), while the yield of P_S increased with the increase of the initial concentration of peroxidase as shown in Fig. 5. Apparently, a higher yield can be obtained if the initial concentration of peroxidase is further increased. Corresponding to this work, the sulfoxidation catalyzed by SPP in the CTAB/isooctane/n-butyl alcohol/water microemulsion is better than in water or organic solvents in which the substrate and product are well dissolved while SPP is in water core. For each enzyme, there is an optimal Wo which makes the enzyme catalytic reaction rate reach the maximum. The enzyme catalytic reaction rate in some microemulsion system is even far higher than that in water, which is called super activity[60,61]. An excellent substrate solubility may help to improve the enzyme catalytic activation dramatically[62]. The relationship between the enzyme activity and Wo generally conforms to the bell-curve in the microemulsion. The optimal Wo means that the water core size of the water-in-oil microemulsions is compatible with the size of the enzyme molecules. When Wo is very small, most of the enzyme molecules cannot be solubilized in the water core of the water-in-oil microemulsion, but are inactivated directly in organic solvents. When

Wo is larger, the enzyme activity decreases with the increase of Wo, as may be due to the increase of water content in the microemulsion[63,64].

As shown in Figs. 2 and 3, the kinetic model established fits the experimental data satisfactorily, the average relative deviation between simulated values and experimental data was 5.44%, and the maximum, 57.68%, respectively. The maximum relative deviation appeared at the lowest yield of product P_S, where the simulated value was 4.4%, and the experimental, 1.86%, thus the deviation was 57.72%. The large relative deviation, therefore, does not mean that the kinetic model does not fit the experimental data well. Furthermore, the distribution of the deviation data was about zero-axis symmetry (data not shown), confirming further that the fitting of the model to test data very well, demonstrating that the mechanism proposed may be reasonable and acceptable. The reaction mechanism proposed involves seven concomitant reactions as mentioned above Reactions 1, 2 and 4 were proven by the labeling experiments in which most ^{18}O, up to 93% incorporation of oxygen into sulfoxides, comes from $H_2{}^{18}O_2$[13,65,66] and reactions 6 and 7 were confirmed by the experiments in which the small amount of ^{18}O transfers from water to thioanisoles[67]. Reactions 1, and 3-7 were also demonstrated by the experimental results of transient-state kinetics[32]. The occurrence of all seven reactions was probed by a variety of spectroscopic methods[47–50].

Due to the complexity of the oxidation catalyzed by peroxidase, the reaction mechanism has been studied by many researchers over the years. Two reaction mechanisms for oxygen transfer to the sulfide were proposed as follows: (1) there are two reactions which are the same as reactions 1 and 2 in Scheme 2, which is a two-electron oxidation mode and (2) there are three reactions which are the same as reactions 1,3 and 4 in Scheme 2[8]. Elizabeth et al[9]. preferred mechanism 2 after the mechanism of S-oxidation to produce (S)-sulfoxide catalyzed by soybean hull sulfoxidase was probed, and the occurrence of mechanism 1, however, could not be excluded from their results. Ubaldo et al[32]. considered three possible mechanisms for the oxidation of sulfides to form sulfoxides mediated by peroxidase as follows: (1) a

mechanism involves two reactions which are same as reactions 1 and 2 in Scheme 2, belonging to an oxene mechanism where a two-electron reduction of HRP-I occurs through a single-step oxygen atom transfer to the sulfides. (2) a reaction system is composed of three reactions which are same as reactions 1, 3 and 4 in Scheme 2, which involves two-step reaction: (i) a single-electron transfer to HRP-I with accompanied by forming of a sulfur cation radical, and (ii) then oxygen anion or hydroxyl radical transfer from HRP-II, which is put forward for S-oxidation catalyzed by cytochrome P-450 first[68]. (3) a mechanism involves reactions 1,3 and 5 in Scheme 2, where cation radicals are produced via the reaction of thioanisole with both HRP-I and HRP-II[13]. The cation radicals produced are followed by disproportionation to form 1 molecule of sulfide and a dication in reaction 6 in Scheme 2, and the dication then reacts with water to form the sulfoxide in reaction 7 in Scheme 2. The transfer of oxygen atom from water to HRP-II has been confirmed by labeling experiments for ^{18}O transfer from water[67]. Ubaldo et al[32] preferred the mechanism involves reactions 1,3 and 5 because the labeling experiments show that most ^{18}O comes from hydrogen peroxide[13].

Samuni et al[46] suggested that the oxidation of HXs mediated by HRP normally proceeds via three concomitant reactions similar to the reactions 1, 3 and 5 in Scheme 2, where HRP reduces peroxide to form HRP-I which is further reduced to HRP-II. Danni et al[47] and Li et al[45] thought that the catalysis by HRP occurs concomitantly via three reactions similar to reactions 1, 2 and 4 in Scheme 2.

Combined research results in the present study with other researchers mentioned above, it can safely draw a conclusion that the mechanism with a two-electron reduction of SPP-I is accompanied by that with a single-electron transfer to SPP-I and nonenzymatic reactions. In other words, the three concomitant submechanisms work to contribute to the asymmetric oxidation, involving five enzymatic and two nonenzymatic reactions, and SPP-I and SPP-II, which is reasonable and can represent the asymmetric oxidation of organic sulfides (thioethers) catalyzed by SPP in the water-in-oil microemulsion. The sub-mechanism with a two-electron reduction is

composed of reactions 1 and 2 in Scheme 2, while the sub-mechanism with a single-electron transfer, reactions 1, 3, 4 and 5, and nonenzymatic reactions involves reactions 6 and 7.

This work has also confirmed the feasibility of SPP as a lower cost and higher thermal stability substitute for HRP in enzymatic catalyzed reactions for the production of various polymers and chemicals including enantiopure sulfoxides.

4.3 Enantioselectivity of SPP in the water-in-oil microemulsion

The e.e was 96.08%, indicating that the asymmetric oxidation of the thioether catalyzed by SPP is highly enantioselective, thus, SPP exhibits excellent enantioselectivity with favor S configuration in the microemulsion. As shown in Scheme 2, thioethers are asymmetrically oxidized catalyzed by SPP to form chiral sulfoxides in reactions 2 and 4 with a preference for S configuration, but racemic products are formed in reaction 7 because the reaction is a nonenzymatic reaction and no enantioselective. As shown in Fig. 4, among reactions 2, 4 and 7, reaction 2 contributed the most to the output of P_S, followed by reaction 4, while reaction 7 was very small, Thus the e.e of the sulfoxide are the result of three concomitant reactions.

The enzymatic oxidation of sulfides catalyzed by soybean hull sulfoxidase in buffer was conducted to yield (S)-sulfoxides with about 90% e.e[9], which is different from earlier studies with no chirality[13,24], the oxidation of thioethers catalyzed by HRP has significant enantioselectivity, and (S)-sulfoxide is about ***5*** times more than (R) -sulfoxide catalyzed by HRP at both pH 7.0 and 4.5 with the (S)-sulfoxides in 60-70% of e.e[65].

Solvent has a great influence on the configuration preference of peroxidase. The asymmetric oxidation of thioamidines catalyzed by SHP favors S configuration in water, whereas R configuration in organic solvents[62]. The enantioselective favor of SPP was S configuration in the present study in water-in-oil microemulsions in which SPP is in an aqueous environment, not organic solvent, so its enantioselective favor should be the same as in water. The performance of SPP may be different from only

water or organic solvents due to the microemulsion including both water and organic solvents.

When thioamidines were oxidized to sulfoxides by chloroperoxidase, the e.e of sulfoxides depends on the properties of oxidant and substrate. When different oxidant and substrate were employed, the e.e changed from 0 to 92% with R absolute configuration[69], which is different from SPP.

4.4 Analysis of the kinetic model

Table 1

Kinetic Paramenters Estimated.

Notation	Parameter		Dimension
K_1	K_1	0	dimensionless
K_2	K_2	34.48	mM^{-1}
K_3	K_3	0.225	mM^{-1}
K_4	K_4	0.051	mM^{-2}
K_5	K_5	5.767	mM^{-2}
K_6	K_6	436.61	mM^{-1}
K_7	K_7	0.03	mM^{-2}
K_8	K_8	0.86	mM^{-3}
k_9	K_9	213.09	$h^{-1}\ U^{-1}ml\ mM^{1-2K10}$
n_1	K_{10}	1.78	dimensionless
k_1	K_{11}	0.015	$h^{-1}\ U^{-1}ml\ mM^{-2}$
k_2	K_{12}	0.028	$h^{-1}\ U^{-1}ml\ mM^{-1}$
k_3	K_{13}	0.0043	$h^{-1}\ U^{-1}ml\ mM^{-2}$
k_4	K_{14}	0.13	$h^{-1}\ U^{-1}ml\ mM^{-1}$
k_5	K_{15}	0.91	$h^{-1}\ U^{-1}ml\ mM^{-2}$
k_6	K_{16}	2.70E-03	$h^{-1}\ U^{-1}ml\ mM^{-1}$
k_7	K_{17}	1.50E-02	$h^{-1}\ U^{-1}ml\ mM^{-2}$
k_8	K_{18}	7.05E-06	$h^{-1}\ U^{-1}ml\ mM^{1-K19}$

n_2	K_{19}	0.20	dimensionless

Table 2

Performances of four kinetic model[1,2].

No	Model	Performance
1	Model prototype, Eqs 8 and 9	Fitting experimental data very well
2	A non-competitive was added to Eqs 8 and 9: $\sum K\times(1+K_i\times Y(1)\times A_0)$	Fitting experimental data poor
3	A non-competitive was added to Eqs 8 and 9: $\sum K\times(1+K_i\times Y(2)\times A_0)$	Fitting experimental data poor
4	A non-competitive was added to Eqs 8 and 9: $\sum K\times(1+K_i\times Y(3)\times A_0)$	Fitting experimental data poor

1 The model equations only have different denominators, but the molecules are the same.

2 The standard to judge whether the model fits well is classified into 4 levels according to average relative deviations between simulated and experimental data as follows, 1: very well(<10%), 2: well(<15%) , 3 some poor(<20%), 4: poor(>20%).

Reaction kinetic constants, revealing the characteristic of reaction mechanisms, are extremely important to understand enzymatic reactions. Table 1 shows the kinetic model parameters of equations (8)-(23). As shown in equation (8) that is actually the denominator of the kinetic equations, independent constant K_1 is zero as displayed in Table 1, which is a typical characteristic of ping-pong mechanism, implying that the kinetic mechanism of the SPP-catalyzed sulfoxidation in water-in-oil microemulsions may follow ping-pong mechanism, but not a sequential mechanism in which K_1 should not be zero. Considering the following two characteristics: K_1 is zero and there is a leaving group, it can be concluded with certainty that the SPP-catalyzed sulfoxidation follows the ping-pong mechanism.

Enzymatic reactions suffer often from the substrate and product inhibition[38,42,51,52]. In this study, the substrate and product inhibition appeared. $K_5\times Y(1)\times A_0\times Y(1)\times A_0$ and $K_7\times Y(2)\times B_0\times Y(2)\times B_0$ represent the substrate inhibition items for H_2O_2 and omeprazole thioether, respectively. As shown in Table 1, K_5 is

large, indicating that H_2O_2 has significant substrate inhibition on the enzymatic sulfoxidation, and in fact, H_2O_2 is unfavorable for peroxidases[54,55]. On the contrary, K_7 is very small, meaning that the substrate inhibition of omeprazole thioether can be ignored. $K_6 \times Y(3) \times B_0$ expresses the product inhibition item for Ps that is larger, implying that Ps have significant product inhibition on the sulfoxidation.

The kinetic model can provide analysis and details of the reaction process, such as enantioselectivity. K_{14} and K_{16} are the kinetic rate constants for the formation of P_S and P_R in equation 2, respectively. As seen from Table 1, K_{14} is far greater than K_{16}, which means that the rate of P_S formation is far greater than P_R in reaction 2. Similarly, for K_{15} and K_{17} which are the kinetic rate constants for the formation of P_S and P_R in equation 4, respectively, it can be concluded that the rate of P_S formation is far greater than P_R in reaction 4. Thus SPP exhibits excellent enantioselectivity, resulting in a high e.e of 96.08%.

When establishing the kinetic model, other situations, such as non-competitive inhibition were considered. Table 2 displays the performances of four kinetic models in which only the model prototype, i.e. equations 8 and 9 fitted experimental data very well. Equations 8 and 9 are denominators of kinetic equations 13-23, and the molecules of the kinetic equations were the same. Other models with a non-competitive inhibition term fitted experimental data poor, indicating that the non-competitive inhibition was not suitable for the SPP-catalyzed sulfoxidation.

5.Conclusions

The asymmetric sulfoxidation catalyzed by SPP were carried out with the esomeprazole yield of 91.56% and e.e of 96.08% The mechanism with a two-electron reduction of SPP-I is accompanied by that with a single-electron transfer to SPP-I and nonenzymatic reactions. With 5.44% of the average relative deviation, a kinetic model fitting experimental data very well was developed, and the enzymatic reactions may follow ping-pong mechanism. This work has also confirmed the feasibility of SPP as a substitute with lower cost and higher thermal stability for HRP in enzymatic

catalyzed reactions for the production of various polymers and chemicals including enantiopure sulfoxides with excellent enantioselectivity.

Credit authorship contribution statement

Yuanyuan Zhang: Conceptualization, Modeling, Writing-original draft, Writing - review & editing, Funding acquisition. **Huiling Li:** Experiment, Optimization, Validation. **Zhiyong Wang:** Experiment, Assay, Modeling. **Depeng Li:** Experiment, Assay, Investigation. **Xin Gao:** Modeling, Writing - review.

Declaration of Competing Interest

The authors declare that they have no known competing financial interests or personal relationships that could have appeared to influence the work reported in this paper.

Acknowledgements

The authors gratefully acknowledge financial support from China Scholarship Council (grant number: 201908370079) and Shandong Provincial Key R&D Program [grant numbers 2019GSF107027, 2019GNC106028 and 2019GSF107033].

Nomenclature

A hydrogen peroxide

A_0 Initial concentration of hydrogen peroxide, mM

B 5-methoxy-2-(((4-methoxy-3,5-dimethylpyridin-2-yl)methyl)thio)-1H-benzoimidazole, Omeprazole thioether,

5-methoxy-2-(((4-methoxy-3,5-dimethylpyridin-2-yl)methyl)thio)-1H-benzo[d]imidazole

B_0 Initial concentration of B, mM

C Cation radical of B, Omeprazole sulfide cation

E_0 Initial concentration of peroxidase, U ml^{-1}

e.e Enantiomeric excess, %

K_1, K_{10}, K_{19} Kinetic parameter, dimensionless

K_2, K_3, K_6 Kinetic parameter, mM^{-1}

K_4, K_5, K_7 Kinetic parameter, mM^{-2}

K_8 Kinetic parameter, mM^{-3}

K_9 Kinetic parameter, h^{-1} U^{-1}ml mM^{1-2K10}

K_{12}, K_{14}, K_{16} Kinetic parameter, h^{-1} U^{-1}ml mM^{-1}

K_{11}, K_{13}, K_{15}, K_{17} Kinetic parameter, h^{-1} U^{-1}ml mM^{-2}

K_{18} Kinetic parameter, h^{-1} U^{-1}ml mM^{1-K19}

KK1, KK2 $\sum K$, sum of Kappa constant, dimensionless

P_R (R)-enantiomer of P

P_S (S)-enantiomer of P, esomeprazole

P 5-Methoxy-2-[(4-methoxy-3,5-dimethylpyridin-2-yl)methylsulfinyl]-1H-benzoimidazole, Omeprazole

Q H_2O

R dication radical of B

Y(i) Relative residual or yield of A, B, P_S , P_R, C and R, for i=1-6, respectively, dimensionless

Y^{simul}_{ij} Simulated residual or yield of A, B, P_S and P_R, for i=1-4, j=1-12, dimensionless

Y^{exp}_{ij} Experimental residual or yield of A, B, P_S and P_R, for i=1-4, j=1-12, dimensionless

t Time, hour

References

(1) Kong, M.; Wang, K.; Dong, R.; Gao, H. Enzyme Catalytic Nitration of Aromatic Compounds. *Enzyme Microb. Technol.* **2015**, *73–74*, 34–43. https://doi.org/10.1016/j.enzmictec.2015.03.008.

(2) Kedderis, G. L.; Koop, D. R.; Hollenberg, P. F. N-Demethylation Reactions Catalyzed by Chloroperoxidase. *J. Biol. Chem.* **1980**, *255* (21), 10174–10182.

(3) Morozov, A. N.; Chatfield, D. C. Chloroperoxidase-Catalyzed

Epoxidation of Cis -β-Methylstyrene: Distal Pocket Flexibility Tunes Catalytic Reactivity. *J. Phys. Chem. B* **2012**, *116* (43), 12905–12914. https://doi.org/10.1021/jp302763h.

(4) Dong, S.; Mao, L.; Luo, S.; Zhou, L.; Feng, Y.; Gao, S. Comparison of Lignin Peroxidase and Horseradish Peroxidase for Catalyzing the Removal of Nonylphenol from Water. *Environ. Sci. Pollut. Res.* **2014**, *21* (3), 2358–2366. https://doi.org/10.1007/s11356-013-2161-4.

(5) Bolzacchini, E.; Brunow, G.; Meinardi, S.; Orlandi, M.; Rindone, B.; Rummakko, P.; Setala, H. Enantioselective Synthesis of a Benzofuranic Neolignan by Oxidative Coupling. *Tetrahedron Lett.* **1998**, *39* (20), 3291–3294. https://doi.org/10.1016/S0040-4039(98)00473-0.

(6) Budde, C. L.; Beyer, A.; Munir, I. Z.; Dordick, J. S.; Khmelnitsky, Y. L. Enzymatic Nitration of Phenols. *J. Mol. Catal. - B Enzym.* **2001**, *15* (1–3), 55–64. https://doi.org/10.1016/S1381-1177(01)00004-2.

(7) Yoshida, K.; Kaothien, P.; Matsui, T.; Kawaoka, A.; Shinmyo, A. Molecular Biology and Application of Plant Peroxidase Genes. *Appl. Microbiol. Biotechnol.* **2003**, *60* (6), 665–670. https://doi.org/10.1007/s00253-002-1157-7.

(8) Ortiz de Montellano, P. R. Control of the Catalytic Activity of Prosthetic Heme by the Structure of Hemoproteins. *Acc. Chem. Res.* **1987**, *20* (8), 289–294. https://doi.org/10.1021/ar00140a004.

(9) Blée, E.; Schuber, F. Mechanism of S-Oxidation Reactions Catalyzed by a Soybean Hydroperoxide-Dependent Oxygenase. *Biochemistry* **1989**, *28* (12), 4962–4967. https://doi.org/10.1021/bi00438a009.

(10) Singh, P.; Prakash, R.; Shah, K. Effect of Organic Solvents on Peroxidases from Rice and Horseradish: Prospects for Enzyme Based Applications. *Talanta* **2012**, *97*, 204–210. https://doi.org/10.1016/j.talanta.2012.04.018.

(11) Watanabe, Y.; Iyanagi, T.; Oae, S. Kinetic Study on Enzymatic S-Oxygenation Promoted by a Reconstituted System with Purified Cytochrome

P-450. *Tetrahedron Lett.* **1980**, *21* (38), 3685–3688. https://doi.org/10.1016/S0040-4039(00)78745-4.

(12) Doerge, D. R. Oxygenation of Organosulfur Compounds by Peroxidases: Evidence of an Electron Transfer Mechanism for Lactoperoxidase. *Arch. Biochem. Biophys.* **1986**, *244* (2), 678–685. https://doi.org/10.1016/0003-9861(86)90636-3.

(13) Kobayashi, S.; Nakano, M.; Kimura, T.; Schaap, A. P. On the Mechanism of the Peroxidase-Catalyzed Oxygen-Transfer Reaction. *Biochemistry* **1987**, *26* (16), 5019–5022. https://doi.org/10.1021/bi00390a020.

(14) Pai, V.; Pai, N. Recent Advances in Chirally Pure Proton Pump Inhibitors. *J. Indian Med. Assoc.* **2007**, *105* (8), 469–474.

(15) Andersson, T.; Weidolf, L. Stereoselective Disposition of Proton Pump Inhibitors. *Clin. Drug Investig.* **2008**, *28* (5), 263–279. https://doi.org/10.2165/00044011-200828050-00001.

(16) Adam, W.; Korb, M. N.; Roschmann, K. J.; Saha-Möller, C. R. Titanium-Catalyzed, Asymmetric Sulfoxidation of Alkyl Aryl Sulfides with Optically Active Hydroperoxides. *J. Org. Chem.* **1998**, *63* (10), 3423–3428. https://doi.org/10.1021/jo980243y.

(17) Dembitsky, V. M. Oxidation, Epoxidation and Sulfoxidation Reactions Catalysed by Haloperoxidases. *Tetrahedron* **2003**, *59* (26), 4701–4720. https://doi.org/10.1016/S0040-4020(03)00701-4.

(18) Kamerbeek, N. M.; Olsthoorn, A. J. J.; Fraaije, M. W.; Janssen, D. B. Substrate Specificity and Enantioselectivity of 4-Hydroxyacetophenone Monooxygenase. *Appl. Environ. Microbiol.* **2003**, *69* (1), 419–426. https://doi.org/10.1128/AEM.69.1.419-426.2003.

(19) Zambianchi, F.; Fraaije, M. W.; Carrea, G.; De Gonzalo; Rodríguez, C.; Gotor, V.; Ottolina, G. Titration and Assignment of Residues That Regulate the Enantioselectivity of Phenylacetone Monooxygenase. *Adv. Synth. Catal.* **2007**, *349* (8–9), 1327–1331. https://doi.org/10.1002/adsc.200600598.

(20) Li, A. T.; Yu, H. L.; Pan, J.; Zhang, J. D.; Xu, J. H.; Lin, G. Q.

Resolution of Racemic Sulfoxides with High Productivity and Enantioselectivity by a Rhodococcus Sp. Strain as an Alternative to Biooxidation of Prochiral Sulfides for Efficient Production of Enantiopure Sulfoxides. *Bioresour. Technol.* **2011**, *102* (2), 1537–1542. https://doi.org/10.1016/j.biortech.2010.08.025.

(21) Zhang, Y.; Liu, F.; Xu, N.; Wu, Y. Q.; Zheng, Y. C.; Zhao, Q.; Lin, G.; Yu, H. L.; Xu, J. H. Discovery of Two Native Baeyer-Villiger Monooxygenases for Asymmetric Synthesis of Bulky Chiral Sulfoxides. *Appl. Environ. Microbiol.* **2018**, *84* (14), e00638-18. https://doi.org/10.1128/AEM.00638-18.

(22) Zhang, Y.; Wu, Y. Q.; Xu, N.; Zhao, Q.; Yu, H. L.; Xu, J. H. Engineering of Cyclohexanone Monooxygenase for the Enantioselective Synthesis of (S)-Omeprazole. *ACS Sustain. Chem. Eng.* **2019**, *7* (7), 7218–7226. https://doi.org/10.1021/acssuschemeng.9b00224.

(23) Van Deurzen, M. P. J.; Van Rantwijk, F.; Sheldon, R. A. Selective Oxidations Catalyzed by Peroxidases. *Tetrahedron* **1997**, *53* (39), 13183–13220. https://doi.org/10.1016/S0040-4020(97)00477-8.

(24) Colonna, S.; Gaggero, N.; Richelmi, C.; Pasta, P. Recent Biotechnological Developments in the Use of Peroxidases. *Trends Biotechnol.* **1999**, *17* (4), 163–168. https://doi.org/10.1016/S0167-7799(98)01288-8.

(25) Adam, W.; Heckel, F.; Saha-Möller, C. R.; Schreier, P. Biocatalytic Synthesis of Optically Active Oxyfunctionalized Building Blocks with Enzymes, Chemoenzymes and Microorganisms. *J. Organomet. Chem.* **2002**, *661* (1–2), 17–29. https://doi.org/10.1016/S0022-328X(02)01805-3.

(26) Dzyuba, S. V.; Klibanov, A. M. Asymmetric Thiosulfinations Catalyzed by Bovine Serum Albumin and Horseradish Peroxidase. *Biotechnol. Lett.* **2003**, *25* (23), 1961–1965. https://doi.org/10.1023/B:BILE.0000004385.50406.06.

(27) Paul, B. K.; Moulik, S. P. Microemulsions: An Overview. *J. Dispers. Sci. Technol.* **1997**, *18* (4), 301–367.

(28) López-Quintela, M. A.; Tojo, C.; Blanco, M. C.; García Rio, L.; Leis, J. R. Microemulsion Dynamics and Reactions in Microemulsions. *Curr. Opin. Colloid Interface Sci.* **2004**, *9* (3–4), 264–278. https://doi.org/10.1016/j.cocis.2004.05.029.

(29) Lopez, F.; Cinelli, G.; Colella, M.; De Leonardis, A.; Palazzo, G.; Ambrosone, L. The Role of Microemulsions in Lipase-Catalyzed Hydrolysis Reactions. *Biotechnol. Prog.* **2014**, *30* (2), 360–366. https://doi.org/10.1002/btpr.1892.

(30) Lopez, F.; Cinelli, G.; Ambrosone, L.; Colafemmina, G.; Ceglie, A.; Palazzo, G. Role of the Cosurfactant in Water-in-Oil Microemulsion: Interfacial Properties Tune the Enzymatic Activity of Lipase. *Colloids Surfaces A Physicochem. Eng. Asp.* **2004**, *237* (1–3), 49–59. https://doi.org/10.1016/j.colsurfa.2004.01.027.

(31) Lopez, F.; Palazzo, G.; Colafemmina, G.; Cinelli, G.; Ambrosone, L.; Ceglie, A. Enzymatic Activity of Lipase Entrapped in CTAB/Water/Pentanol/Hexane Reverse Micelles: A Functional and Microstructural Investigations. In *Progress in Colloid and Polymer Science*; Springer, 2004; Vol. 123, pp 174–177. https://doi.org/10.1007/b11756.

(32) Perez, U.; Brian Dunford, H. Transient-State Kinetics of the Reactions of l-Methoxy-4-(Methylthio)Benzene with Horseradish Peroxidase Compounds I and II. *Biochemistry* **1990**, *29* (11), 2757–2763. https://doi.org/10.1021/bi00463a019.

(33) Hong, E. S.; Kwon, O. Y.; Ryu, K. Strong Substrate-Stabilizing Effect of a Water-Miscible Ionic Liquid [BMIM][BF4] in the Catalysis of Horseradish Peroxidase. *Biotechnol. Lett.* **2008**, *30* (3), 529–533. https://doi.org/10.1007/s10529-007-9570-8.

(34) Lee, Y. M.; Kwon, O. Y.; Yoo, I. K.; Ryu, K. G. Effect of Ionic Liquid on the Kinetics of Peroxidase Catalysis. *J. Microbiol. Biotechnol.* **2007**, *17* (4), 600–603.

(35) Bornadel, A.; Åkerman, C. O.; Adlercreutz, P.; Hatti-Kaul, R.; Borg,

N. Kinetic Modeling of Lipase-Catalyzed Esterification Reaction between Oleic Acid and Trimethylolpropane: A Simplified Model for Multi-Substrate Multi-Product Ping-Pong Mechanisms. *Biotechnol. Prog.* **2013**, *29* (6), 1422–1429. https://doi.org/10.1002/btpr.1806.

(36) Mathpati, A. C.; Badgujar, K. C.; Bhanage, B. M. Kinetic Modeling and Docking Study of Immobilized Lipase Catalyzed Synthesis of Furfuryl Acetate. *Enzyme Microb. Technol.* **2016**, *84*, 1–10. https://doi.org/10.1016/j.enzmictec.2015.12.003.

(37) Kamble, M. P.; Shinde, S. D.; Yadav, G. D. Kinetic Resolution of (R,S)-α-Tetralol Catalyzed by Crosslinked Candida Antarctica Lipase B Enzyme Supported on Mesocellular Foam: A Nanoscale Enzyme Reactor Approach. *J. Mol. Catal. B Enzym.* **2016**, *132*, 61–66. https://doi.org/10.1016/j.molcatb.2016.06.013.

(38) Zhang, Y.; Zhao, Y.; Jiang, W.; Yao, Q.; Li, Z.; Gao, X.; Liu, T.; Yang, F.; Wang, F.; Liu, J. Lipase-Catalyzed Oxidation of Cyclohexanone to Form ϵ-Caprolactone and Kinetic Modeling. *ACS Sustain. Chem. Eng.* **2019**, *7* (15), 13294–13306. https://doi.org/10.1021/acssuschemeng.9b02521.

(39) Yadav, G. D.; Trivedi, A. H. Kinetic Modeling of Immobilized-Lipase Catalyzed Transesterification of n-Octanol with Vinyl Acetate in Non-Aqueous Media. *Enzyme Microb. Technol.* **2003**, *32* (7), 783–789. https://doi.org/10.1016/S0141-0229(03)00064-4.

(40) Badgujar, K. C.; Bhanage, B. M. Synthesis of Geranyl Acetate in Non-Aqueous Media Using Immobilized Pseudomonas Cepacia Lipase on Biodegradable Polymer Film: Kinetic Modelling and Chain Length Effect Study. *Process Biochem.* **2014**, *49* (8), 1304–1313. https://doi.org/10.1016/j.procbio.2014.04.014.

(41) Yadav, G. D.; Borkar, I. V. Kinetic Modeling of Immobilized Lipase Catalysis in Synthesis of n -Butyl Levulinate. *Ind. Eng. Chem. Res.* **2008**, *47* (10), 3358–3363. https://doi.org/10.1021/ie800193f.

(42) Zhang, Y.; Zhao, Y.; Gao, X.; Jiang, W.; Li, Z.; Yao, Q.; Yang, F.;

Wang, F.; Liu, J. Kinetic Model of the Enzymatic Michael Addition for Synthesis of Mitomycin Analogs Catalyzed by Immobilized Lipase from T. Laibacchii. *Mol. Catal.* **2019**, *466*, 146–156. https://doi.org/10.1016/j.mcat.2019.01.017.

(43) Blake, R. C.; Coon, M. J. On the Mechanism of Action of Cytochrome P-450. Spectral Intermediates in the Reaction of P-450LM2 with Peroxy Compounds. *J. Biol. Chem.* **1980**, *255* (9), 4100–4111.

(44) Wagner, G. C.; Palcic, M. M.; Dunford, H. B. Absorption Spectra of Cytochrome P450CAM in the Reaction with Peroxy Acids. *FEBS Lett.* **1983**, *156* (2), 244–248. https://doi.org/10.1016/0014-5793(83)80505-5.

(45) Ji, L.; Franke, A.; Brindell, M.; Oszajca, M.; Zahl, A.; Van Eldik, R. Combined Experimental and Theoretical Study on the Reactivity of Compounds I and II in Horseradish Peroxidase Biomimetics. *Chem. - A Eur. J.* **2014**, *20* (44), 14437–14450. https://doi.org/10.1002/chem.201402347.

(46) Samuni, U.; Maimon, E.; Goldstein, S. A Kinetic Study of the Oxidation of Hydroxamic Acids by Compounds I and II of Horseradish Peroxidase: Effect of Transition Metal Ions. *J. Coord. Chem.* **2018**, *71* (11–13), 1728–1737. https://doi.org/10.1080/00958972.2018.1493200.

(47) Harris, D. L.; Loew, G. H. Identification of Putative Peroxide Intermediates of Peroxidases by Electronic Structure and Spectra Calculations. *J. Am. Chem. Soc.* **1996**, *118* (43), 10588–10594. https://doi.org/10.1021/ja9617247.

(48) Dunford, H. B. Horseradish Peroxidases: Structure and Kinetic Properties. *Peroxidases Chem. Biol.* **1991**, *2*, 1–24.

(49) Edwards, S. L.; Xuong, N. H.; Hamlin, R. C.; Kraut, J. Crystal Structure of Cytochrome c Peroxidase Compound I. *Biochemistry* **1987**, *26* (6), 1503–1511. https://doi.org/10.1021/bi00380a002.

(50) Fülöp, V.; Phizackerley, R. P.; Soltis, S. M.; Clifton, I. J.; Wakatsuki, S.; Erman, J.; Hajdu, J.; Edwards, S. L. Laue Diffraction Study on the Structure of Cytochrome c Peroxidase Compound I. *Structure* **1994**, *2* (3),

201–208. https://doi.org/10.1016/S0969-2126(00)00021-6.

(51) Waghmare, G. V.; Chatterji, A.; Rathod, V. K. Kinetics of Enzymatic Synthesis of Cinnamyl Butyrate by Immobilized Lipase. *Appl. Biochem. Biotechnol.* **2017**, *183* (3), 792–806. https://doi.org/10.1007/s12010-017-2464-x.

(52) Liu, K. M.; Liu, K. J. Lipase-Catalyzed Synthesis of Palmitanilide: Kinetic Model and Antimicrobial Activity Study. *Enzyme Microb. Technol.* **2016**, *82*, 82–88. https://doi.org/10.1016/j.enzmictec.2015.08.017.

(53) Leskovac, V.; Ebrary, I. *Comprehensive Enzyme Kinetics*; Kluwer Academic Publishers: Boston, 2004. https://doi.org/10.1007/b100340.

(54) Ator, M. A.; David, S. K.; Ortiz de Montellano, P. R. Stabilized Isoporphyrin Intermediates in the Inactivation of Horseradish Peroxidase by Alkylhydrazines. *J. Biol. Chem.* **1989**, *264* (16), 9250–9257.

(55) Goodwin, D. C.; Grover, T. A.; Aust, S. D. Roles of Efficient Substrates in Enhancement of Peroxidase-Catalyzed Oxidations. *Biochemistry* **1997**, *36* (1), 139–147. https://doi.org/10.1021/bi961465y.

(56) Drozdz, A.; Erfurt, K.; Bielas, R.; Chrobok, A. Chemo-Enzymatic Baeyer-Villiger Oxidation in the Presence of Candida Antarctica Lipase B and Ionic Liquids. *New J. Chem.* **2015**, *39* (2), 1315–1321. https://doi.org/10.1039/c4nj01976h.

(57) Törnvall, U.; Hedström, M.; Schillén, K.; Hatti-Kaul, R. Structural, Functional and Chemical Changes in Pseudozyma Antarctica Lipase B on Exposure to Hydrogen Peroxide. *Enferm. Infecc. Microbiol. Clin.* **2010**, *28* (SUPPL. 3), 1867–1875. https://doi.org/10.1016/j.biochi.2010.07.008.

(58) Katritzky, A. R.; Akhmedov, N. G.; Denisko, O. V. 1H and 13C NMR Spectroscopic Study of Oxidation of D,L-Cystine and 3,3′-Dithiobis(Propionic Acid) with Hydrogen Peroxide in Aqueous Solution. *Magn. Reson. Chem.* **2003**, *41* (1), 37–41. https://doi.org/10.1002/mrc.1110.

(59) Törnvall, U.; Fürst, C. M.; Hatti-Kaul, R.; Hedström, M. Mass Spectrometric Analysis of Peptides from an Immobilized Lipase: Focus on

Oxidative Modifications. *Rapid Commun. Mass Spectrom.* **2009**, *23* (18), 2959–2964. https://doi.org/10.1002/rcm.4208.

(60) Carvalho, C. M. L.; Cabral, J. M. S. Reverse Micelles as Reaction Media for Lipases. *Biochimie* **2000**, *82* (11), 1063–1085. https://doi.org/10.1016/S0300-9084(00)01187-1.

(61) Chen, N.; Fan, J. B.; Xiang, J.; Chen, J.; Liang, Y. Enzymatic Hydrolysis of Microcrystalline Cellulose in Reverse Micelles. *Biochim. Biophys. Acta - Proteins Proteomics* **2006**, *1764* (6), 1029–1035. https://doi.org/10.1016/j.bbapap.2006.03.015.

(62) Schoevaart, R.; Van Rantwijk, F.; Sheldon, R. A. Peroxidase-Catalyzed Asymmetric Sulfoxidation in Organic Solvents versus in Water. *Biotechnol. Bioeng.* **2000**, *70* (3), 353–357. https://doi.org/10.1002/1097-0290(20001105)70:3<353::AID-BIT13>3.0.CO;2-0.

(63) Martinek, K.; Klyachko, N. L.; Kabanov, A. V.; Khmelnitsky, Y. L.; Levashov, A. V. Micellar Enzymology: Its Relation to Membranology. *BBA - Biomembr.* **1989**, *981* (2), 161–172. https://doi.org/10.1016/0005-2736(89)90024-2.

(64) Bru, R.; Sanchez-Ferrer, A.; Garcia-Carmona, F. Kinetic Models in Reverse Micelles. *Biochem. J.* **1995**, *310* (3), 721–739. https://doi.org/10.1042/bj3100721.

(65) Harris, R. Z.; Newmyer, S. L.; De Montellano, P. R. O. Horseradish Peroxidase-Catalyzed Two-Electron Oxidations. Oxidation of Iodide, Thioanisoles, and Phenols at Distinct Sites. *J. Biol. Chem.* **1993**, *268* (3), 1637–1645.

(66) Doerge, D. R.; Cooray, N. M.; Brewster, M. E. Peroxidase-Catalyzed S-Oxygenation: Mechanism of Oxygen Transfer for Lactoperoxidase. *Biochemistry* **1991**, *30* (37), 8960–8964. https://doi.org/10.1021/bi00101a007.

(67) Hashimoto, S.; Tatsuno, Y.; Kitagawa, T. Resonance Raman Evidence for Oxygen Exchange between the Fe(IV)=O Heme and Bulk Water

during Enzymic Catalysis of Horseradish Peroxidase and Its Relation with the Heme-Linked Ionization. *Proc. Natl. Acad. Sci. U. S. A.* **1986**, *83* (8), 2417–2421. https://doi.org/10.1073/pnas.83.8.2417.

(68) Watanabe, Y.; Numata, T.; Iyanagi, T.; Oae, S. Enzymatic Oxidation of Alkyl Sulfides by Cytochrome P-450 and Hydroxyl Radical. *Bull. Chem. Soc. Jpn.* **1981**, *54* (4), 1163–1170. https://doi.org/10.1246/bcsj.54.1163.

(69) Colonna, S.; Gaggero, N.; Manfredi, A.; Casella, L.; Gullotti, M.; Carrea, G.; Pasta, P. Enantioselective Oxidations of Sulfides Catalyzed by Chloroperoxidase. *Biochemistry* **1990**, *29* (46), 10465–10468. https://doi.org/10.1021/bi00498a006.